Published in final edited form as:
Mol Cell. 2016 April 21; 62(2): 307–313. doi:10.1016/j.molcel.2016.03.006.

A genomewide CRISPR screen identifies CDC25A as a determinant of sensitivity to ATR inhibitors

Sergio Ruiz[1,*], **Cristina Mayor-Ruiz**[1,*], **Vanesa Lafarga**[1], **Matilde Murga**[1], **Maria Vega-Sendino**[1], **Sagrario Ortega**[2], and **Oscar Fernandez-Capetillo**[1,3]

[1]Genomic Instability Group, Spanish National Cancer Research Centre (CNIO), Madrid 28029, Spain

[2]Transgenics Unit, Spanish National Cancer Research Centre (CNIO), Madrid 28029, Spain

[3]Science for Life Laboratory, Division of Translational Medicine and Chemical Biology, Department of Medical Biochemistry and Biophysics, Karolinska Institute, S-171 21 Stockholm, Sweden

Summary

One recurring theme in drug development is to exploit synthetic lethal properties as means to preferentially damage the DNA of cancer cells. Others and we have previously developed inhibitors of the ATR kinase, and shown are particularly genotoxic for cells expressing certain oncogenes. In contrast, the mechanisms of resistance to ATR inhibitors remain unexplored. We here report on a genomewide CRISPR-Cas9 screen, which identified CDC25A as a major determinant of sensitivity to ATR inhibition. CDC25A deficient cells resist high doses of ATR inhibitors, which we show is due to their failure to prematurely enter mitosis in response to the drugs. Forcing mitotic entry with WEE1 inhibitors restores the toxicity of ATR inhibitors in CDC25A deficient cells. With ATR inhibitors now entering the clinic, our work provides a better understanding of the mechanisms by which these compounds kill cells, and reveals genetic interactions that could be used for their rational use.

Introduction

Targeting DNA repair enzymes is an active area of drug development in cancer therapy. The interest was fueled by the discovery of synthetic lethal interactions, such as the selective toxicity of polyADP-rybosil transferase (PARP) inhibitors for cells lacking *BRCA* tumor suppressors (Bryant et al., 2005; Farmer et al., 2005). One widespread feature of cancer cells is the presence of replication stress (RS), which is driven by the underlying oncogenes and is responsible for a large fraction of the genomic rearrangements found in cancer cells

Correspondence: S.R. (sruizm@cnio.es) or O.F. (ofernandez@cnio.es), **Contact Info.**: Oscar Fernandez-Capetillo or Sergio Ruiz, Spanish National Cancer Research Centre (CNIO), Melchor Fernandez Almagro, 3, Madrid 28029, Spain, Tel.: +34.91.732.8000 Ext: 3480, Fax: +34.91.732.8028.
*Co-first authors

Author Contributions

C.M. and S.R. designed and participated in most of the experiments of this study. V.L. performed DNA replication analyses. M.M. performed CDC25A overexpression experiments. M.V. provided technical help. S.O. helped in the generation of ES^{Cas9} cells. O.F. and S.R. coordinated the study and wrote the MS.

The authors declare no competing financial interests.

Europe PMC Funders Author Manuscripts

(Halazonetis et al., 2008; Lecona and Fernandez-Capetillo, 2014). RS stands for the accumulation of ssDNA at stalled replication forks, which can promote the nucleolytic breakage of the fork and subsequent recombination events, as well as overall replication catastrophe through the exhaustion of ssDNA-binding proteins (Toledo et al., 2013). In mammals, RS is sensed and suppressed by a signaling-cascade initiated by the ATR kinase (Cimprich and Cortez, 2008; Lopez-Contreras and Fernandez-Capetillo, 2010). Recent evidence has also revealed the existence of a backup pathway controlled by DNAPK and CHK1 kinases that limits ssDNA in conditions of limited ATR activity (Buisson et al., 2015). We previously hypothesized that targeting ATR should be particularly deleterious for cancer cells experiencing high levels of oncogene-induced RS. Accordingly, mice with reduced ATR levels are refractory to the development of various tumors (Murga et al., 2011; Schoppy et al., 2012), and ATR inhibitors are preferentially toxic for cells expressing MYC or CYCE oncogenes, or lacking tumor suppressors such as ATM or P53 (Kwok et al., 2015; Reaper et al., 2011; Toledo et al., 2011). In addition, other cancer-associated conditions such as the use of the Alternative Lengthening of Telomeres (ALT) pathway for telomere maintenance also increase the sensitivity to ATR inhibitors (Flynn et al., 2015). In contrast to mutations that sensitize to these compounds, whether resistance to ATR inhibitors can occur remains unknown.

Results

In order to develop genomewide CRISPR screens, we first developed murine embryonic stem (ES) cells carrying a doxyciclin (Dox)-inducible Cas9 cDNA (ES^{Cas9}). We used a previously developed system whereby the *Cas9* cDNA under the control of a tetracycline responsive operator (tetO) was placed at the 3' untranslated region of the ubiquitously expressed *Col1a1* locus, and the expression of the rtTA transactivator was driven by the *ROSA26* promoter (Beard et al., 2006) (Figure 1A). This two-tier system provides a stringent expression of Cas9, thereby preventing nuclease activity until Dox addition. Two clones showing a clear Dox-inducible Cas9 expression were selected for further experiments (Figure 1B; Figure S1A,B). To determine the efficiency of CRISPR-Cas9 editing in these cells, we co-infected a clone of ES^{Cas9} cells with lentiviruses expressing green fluorescent protein (GFP) and with lentiviruses expressing both a *Gfp*-targeting sgRNA and blue fluorescent protein (BFP). After sorting and before the addition of Dox, cells expressing both GFP and BFP dominated the culture. 48 hr after Dox the GFP (but not BFP) signal started to decrease and was virtually absent by 5 days of treatment (Figure 1C). To further characterize the efficiency of the system at endogenous loci, 3 different lentiviruses carrying sgRNAs against *P53* were used to independently infect ES^{Cas9} cells. After infection, a Dox-inducible reduction in P53 levels was detectable with all sgRNAs (Figure 1D). Together, these results revealed that ES^{Cas9} cells provide a very efficient platform for obtaining nullyzygous mutations in primary mammalian cells by CRISPR-Cas9 editing and prompted us to conduct forward genetic screenings using this system.

To perform our screenings, we used a recently described library targeting 19.150 mouse genes with 87.897 sgRNAs (Koike-Yusa et al., 2014). ES^{Cas9} cells were infected with the library at a low MOI to enrich in cells carrying a single lentiviral copy and sorted for BFP expression (Figure S1C). Infected cells were subsequently treated with Dox for 10 days to

induce CRISPR-mediated mutations. To confirm the quality of the library and as proof-of-principle, we first conducted a screening for resistance against 6-thioguanine (6TG). 6TG is an inert compound, which is converted to toxic inside cells by the action of hypoxanthine-guanine phosphoribosyltransferase (HPRT). 5 million cells from the mutagenized library were exposed to 20μM 6TG for 7 days, a time/dose at which no wild type (wt) ES^{Cas9} cells survive. 4 out of 5 of the resistant clones that were isolated carried sgRNAs targeting *Hprt* (Table S1). Using this library, a second screening was performed exposing the cells for 9 days to 0.9 μM of an ATR inhibitor developed by our group in a previous chemical screen (ATRi) (Toledo et al., 2011), again a dose and time at which no wt cells survive. A 3-day treatment with 300nM ATRi suffices to kill all wt ES^{Cas9} cells, so that our screening was performed at highly stringent conditions. 5 out of 7 of the resistant clones that could be isolated in this screen carried sgRNAs that targeted the phosphatase CDC25A (Table S1). To strengthen our observations, we generated a new library using an independent clone of ES^{Cas9} cells and repeated the screen. In this case, 6 out of 6 of the 6TG-resistant clones carried sgRNAs targeting *Hprt* (Table S1). As for ATRi, we obtained 16 resistant clones, 6 of which targeted *Cdc25a*. This second library also identified sgRNAs targeting *Cnot8*, a member of the CCR4-NOT deadenylase complex (Collart and Panasenko, 2012), in a large fraction of the resistant clones (6/16) (Table S1). Given the recurrence of *Cdc25a*-targeting sgRNAs in both libraries, we focused this study in understanding the mechanism by which CDC25A deficiency limits the toxicity of ATR inhibitors.

To verify that CDC25A deficiency confers resistance to ATR inhibition we first analyzed CDC25A expression in 3 independent ATRi-resistant clones isolated from the screen. Western blotting revealed the absence of CDC25A protein expression in these cells (Figure 2A), all of which carried small deletions or mutations at the sequence of *Cdc25a* targeted by the sgRNA (Figure 2B). Multiple lines of evidence confirmed a high degree of resistance against ATR inhibitors in CDC25A deficient cells. First, whereas chronic exposure to ATRi kills all wt ES^{Cas9} cells at doses above 300 nM, CDC25A-deficient cells were able to expand at doses up to 3 μM (Figure 2C). XTT viability assays confirmed the resistance of the mutant clones to ATRi (Figure 2D). Moreover, in all clones, CDC25A deficiency also conferred resistance to an independent ATR inhibitor (AZ-20) (Foote et al., 2013) and to the CHK1 inhibitor UCN-01 (Figure S2A). Finally, and to discard any potential off-target effects of the sgRNA identified in the screen, we generated additional CDC25A deficient cells by infecting ES^{Cas9} cells with lentiviruses expressing 4 independent sgRNA sequences targeting *Cdc25a*. After selection, all pools of infected cells acquired resistance to ATRi in response to Dox (Figure S2B). Consistent with our findings in mouse cells, CDC25A heterozygosity in HAP1 cells (Figure S2C-E) or its depletion by siRNA in 5 additional human cancer cell lines (Figure S2F,G) invariably led to resistance to ATRi. Finally, we also tested whether increased CDC25A expression enhanced the sensitivity to ATR inhibition. Indeed, CDC25A overexpression sensitized NIH3T3 cells to ATRi (Figure S2H,I). Moreover, CDC25A expression is highest in tumors which are already known to be particularly dependent on the ATR/CHK1 response such as Burkitt lymphomas, acute lymphoblastic or myeloid leukemias and diffuse large B cell lymphomas (Figure S2J) (Derenzini et al., 2015; Kwok et al., 2015; Murga et al., 2011; Santos et al., 2014; Sarmento

et al., 2015; Schoppy et al., 2012) Together, these results reveal that CDC25A levels determine the sensitivity of mammalian cells to ATR inhibitors.

We next tried to address the mechanism by which loss of CDC25A promoted resistance to ATR inhibitors. First, we evaluated whether ATR inhibition generated RS and/or chromosomal breakage in CDC25A-deficient cells. To determine whether this was the case, we first analyzed replication dynamics in response to ATRi. In vertebrates, depletion of ATR leads to increased origin firing and, as a consequence, slower progression at each individual fork (Eykelenboom et al., 2013). Consistent with an increase in origin firing, chemical inhibition of ATR in ES^{Cas9} cells led to a rapid overall increase in EdU incorporation rates as measured by High-Throughput Microscopy (HTM), which was however not affected by CDC25A deficiency (Figure 3A). Moreover, ATR inhibitors induced equivalent amounts of ssDNA in wt and *Cdc25a*$^{-/-}$ ES^{Cas9} cells (Figure 3B). Next, we monitored the impact of ATR inhibition at individual replication forks by stretched DNA fiber analyses. Despite CDC25A-deficient cells presented a slightly lower density of replication forks in unchallenged conditions, the addition of ATRi increased origin firing and decreased fork rates in both wt and *Cdc25a*$^{-/-}$ ES^{Cas9} cells (Figure S3A,B). Surprisingly, and in contrast to the modest reduction observed in CDC25-deficient ES^{Cas9} cells on the amount of ATRi-induced RS, chromosomal breakage induced by the drug was fully abrogated in *Cdc25a*$^{-/-}$ cells, measured by western blotting against γH2AX and RPA32-S4/8P (Figure 3C), as well as by quantifying γH2AX and 53BP1 nuclear foci by HTM (Figures 3D and S3C). Hence, despite ATR inhibitors generate RS in both wt and mutant cells, this is only translated into cytotoxic DNA double strand breaks (DSBs) in the presence of CDC25A. Whereas we cannot discard that some cell-death might be due to RS instead of DSB, we do not think that an altered RS-response or an intrinsic resistance to RS can account for the resistance to ATRi in CDC25A-deficient cells. Accordingly, *Cdc25a*$^{-/-}$ ES^{Cas9} cells show normal levels of CHK1 phosphorylation upon exposure to the RS-inducing agent hydroxyurea (HU) and are not resistant to this drug (Figure S3D,E).

CDC25A was originally discovered as a mitosis promoting factor (Russell and Nurse, 1986), which promotes M-phase entry by eliminating inhibitory phosphorylations in CDK1 that are placed by the WEE1 kinase (Galaktionov and Beach, 1991). Later studies revealed that, in response to DNA damage, CHK1-dependent phosphorylation of CDC25A targets it for degradation, thereby activating the checkpoints that limit the expansion of damaged cells (Falck et al., 2001; Mailand et al., 2000; Peng et al., 1997; Sanchez et al., 1997). Hence, we first asked whether ATR inhibition would increase CDC25A levels. In fact, exposure to ATRi led to a dose-dependent increase in CDC25A levels in ES^{Cas9} cells (Figure S4A). Noteworthy, whereas we could validate that CNOT8 deficiency renders ES^{Cas9} cells resistant to ATRi, this phenotype was not linked to CDC25A expression (Figure S4B,C).

Recent studies have indicated that the generation of DSBs by RS is due to un-replicated regions of the genome reaching mitosis (reviewed in (Mankouri et al., 2013)). Consistently, FACS analyses revealed that ATRi-induced γH2AX occurred in cells with a late G2/M DNA content, which was again absent in *Cdc25a*$^{-/-}$ ES^{Cas9} cells (Figure 4A). Moreover, immunofluorescence analyses confirmed the presence of ATRi-induced γH2AX foci in mitotic cells, identified by the presence of H3-S10 phosphorylation, in wt but not in

CDC25A-deficient cells (Figure 4B). We thus hypothesized that chromosomal breaks induced by ATR inhibitors could be due to a premature entry into M-phase of cells undergoing RS provoked by an increase of CDC25A levels. Supporting this view, FACS analyses revealed that ATR inhibitors promoted mitotic entry in ES^{Cas9} cells, an effect that was largely abolished in CDC25A-deficient cells (Figure 4C). Noteworthy, a prolonged exposure to ATR inhibitors led to H3-S10 phosphorylation in wt cells with an S-phase DNA content, consistent with the premature activation of the mitotic kinases in cells still undergoing DNA replication. ATR inhibitors also induce some mitotic entry in *Cdc25a*$^{-/-}$ ES^{Cas9} cells, albeit at later times and to a much lesser extent. Thus, whereas CDC25A upregulation is the main responsible for the premature mitotic entry induced by ATRi, ATR also limits mitotic entry through CDC25A-independent mechanisms. In this regard, and given the known roles of the CDC25A homologue CDC25B in the G2/M transition, we tested the impact of CDC25B deficiency in the response to ATR inhibitors. However, ATR inhibition did not increase the levels of CDC25B (Figure S4A), and CDC25B deletion in ES^{Cas9} cells or siRNA-mediated depletion in human cancer cell lines did not increase the resistance to ATR inhibitors (Figure S4D-G). Finally, and to further document how ATR inhibitors induce cell death, we recorded videos of H2B-eGFP expressing wt and *Cdc25a*$^{-/-}$ ES^{Cas9} cells exposed to ATR inhibitors (Figure S4H). These analyses revealed that ATRi-induced cell death occurred frequently at mitosis or shortly during the following interphase. Interestingly, the low levels of cell death that are observed in CDC25A-deficient cells exposed to ATRi also tend to occur after passage through mitosis, suggesting that the same mechanism of ATRi-induced cell killing applies to these cells.

As final proof of this model, we forced mitotic entry in CDC25A-deficient cells by activating CDK1 through WEE1 inhibition. In agreement with our hypothesis, WEE1 inhibitors generated DSB and forced mitotic entry in CDC25A-deficient cells (as measured by H2AX and H3S10 phosphorylation by western blotting) (Figure 4D). Moreover, WEE1 inhibitors sensitized CDC25A-deficient cells to ATR inhibitors (Figure 4E). Both WEE1 and ATR inhibitors reduced the inhibitory phosphorylation of CDK1 at Tyr15, particularly when combined together (Figure S4I). Of note, a prolonged exposure to ATRi reduced CDK1-Y15P levels even in CDC25A-deficient cells, consistent with our earlier observations suggesting that whereas CDC25A plays a central role, ATR can limit mitotic entry through CDC25A-dependent and -independent mechanisms. Altogether, the results presented here suggest that the toxicity of ATR inhibitors is due to a combination of (a) the generation of RS and (b) promoting the premature mitotic entry of cells bearing RS, where DNA breaks arise. Forced mitotic entry is a consequence of the premature activation of CDK1, which is largely mediated by an increase in CDC25A phosphatase levels.

Discussion

We here report on a cellular platform for the development of forward genetic screenings in primary mammalian cells using CRISPR-Cas9, which we have used to identify mechanisms of resistance to ATR inhibitors. Two independent screenings identified sgRNAs targeting *Cdc25a* and *Cnot8* that conferred resistance to these compounds. Whereas this study focused on CDC25A given that it is a well-known oncogene (Ray and Kiyokawa, 2008), we also confirmed the resistance to ATRi in the *Cnot8* mutant clones isolated from the screening;

although to a lesser extent to that observed in CDC25A deficient cells. Given the pleotropic roles of the CCR4-NOT complex on RNA metabolism, its link to ATR biology remains to be determined although it seems independent from CDC25A since ATRi-induced CDC25A upregulation occurs normally in CNOT8-deficient cells (Figure S4C). In what regards to CDC25A, this oncogene is frequently overexpressed in various cancers, which we suggest could confer sensitivity to ATR inhibitors. Whereas reduced levels of CDC25A emerge as a mechanism of resistance to ATR inhibitors in cancer therapy remains to be seen, our findings also suggest that CDC25A levels could be used to identify patients more likely to respond to this therapy. Supporting this view, CDC25A levels correlate with the sensitivity to ATRi in the human cancer cell lines used in this study (Figure S2E,G) and, as mentioned before, CDC25A expression is highest in tumors known to be sensitive to ATRi (Figure S2J).

In what regards to the use of ATR inhibitors for cancer therapy, our work indicates that a combination with WEE1 inhibitors could overcome such a resistance, and suggests the potential of ATRi/WEE1i drug combinations. Along these lines, a recent work has identified that WEE1 inhibitors are preferentially toxic for cancer cells with low levels of the ribonucleotide reductase subunit RRM2 (Prister et al., 2015), which has been recently shown to be key for the essential roles of ATR in mammalian cells (Buisson et al., 2015; Lopez-Contreras et al., 2015). In addition to WEE1 inhibitors, our work suggests that ATR inhibitors should synergize not only with other RS-inducing drugs such as cisplatin or gemcitabine (Prevo et al., 2012; Vendetti et al., 2015), but also with other strategies that promote mitotic entry.

Finally, our work sheds light into the mechanisms of cell killing by ATR inhibitors. The results presented illustrate that the toxicity of these compounds is a combination of two activities: (a) their capacity to induce RS, and (b) to force premature mitotic entry. This second activity is not present in other RS-inducing chemotherapeutic drugs, which might offer an advantage to ATR inhibitors in certain conditions. Bringing cells with RS into mitosis would promote the cleavage of stalled forks and the subsequent generation of toxic DSBs. This model is consistent with recent data showing that RS is converted into DSB during mitosis (Minocherhomji et al., 2015). Interestingly, a prolonged exposure of ATR inhibitors leads to the phosphorylation of mitotic markers such as H3S10 in cells with a DNA content lower than G2 (Figure 4C). Thus, premature mitosis might occur as early as in S-phase, which would support earlier observations of replication catastrophe induced by ATR inhibitors (Toledo et al., 2013).

In summary, our work provides proof-of-principle of the value of ES^{Cas9} cells as an efficient platform for CRISPR-Cas9 based genomewide screenings, clarifies the mechanism by which ATR inhibitors kill cells, and has led to the identification of CDC25A as a potential biomarker to optimize the rational use of ATR inhibitors in cancer therapy.

Experimental Procedures

Generation of ES^{Cas9} cells

The previously described KH2 ES cell line (Beard et al., 2006) contains an frt-flanked neomycin resistance gene and an ATG-less hygromycin resistance gene without promoter at the *Col1a1* locus. In addition, this cell line also contains an M2rtTA transactivator targeted at the endogenous *Rosa26* locus. A Flp-dependent recombination event using the pBS31 plasmid provides a PGK promoter and a ATG initiation codon to the hygromycin gene as well as the gene of interest under a tetO minimal promoter into the *Col1a1* locus. This recombination eliminates the neomycin resistance gene and confers a new resistance to the successfully targeted cell. Thus, to generate the ES^{Cas9} cells, KH2 cells were electroporated with pBS31-Cas9 and a plasmid encoding for Flp. 24-48 hours after electroporation, cells were incubated with 140μg/ml of hygromycin to select cells in which recombination took place. Resistant clones were picked, amplified and tested for Dox-inducible Cas9 expression.

Generation of genomewide mutant libraries and screening

Two independent genomewide mutant libraries were generated with two different ES^{Cas9} clones, as previously described (Koike-Yusa et al., 2014) with minor modifications. Briefly, 5x10^6 ES^{Cas9} cells were infected in suspension for one hour at 37ºC with the genomewide lentiviral library at a MOI (multiplicity of infection) of 0.3 and plated on a fresh layer of feeder cells. Three days after the infection, a total of 2x10^6 BFP-positive cells (estimated library coverage of 20X) were sorted and cultured to establish each of the cell libraries. Next, we maintained a minimum of 5x10^6 cells (estimated library coverage of 50X) with 2 μg/ml of doxycycline for a total of 10 days to induce Cas9 expression allowing gene editing. To perform the 6-thioguanine (6-TG) screening, a total of untreated or doxycycline-treated 5x10^6 cells were incubated with 6-TG at 20μM for 7 days. Resistant clones were picked and amplified on culture media without 6-TG. To perform the ATR inhibitor (ATRi) screening, a total of untreated or doxycycline-treated 5x10^6 mESCs were incubated with ATRi (0.9 μM) for 9 days. Resistant clones were picked and amplified on culture media with ATRi (0.3 μM) for 5 additional days before using culture media without ATRi. The ATRi used in these study was found in a screening reported previously (Toledo et al., 2011). To identify the sgRNA sequences inserted in the resistant mESC clones, we amplified by PCR the fragment flanking the U6-sgRNA cassette from the lentiviral vector, sub-cloned it in a TOPO vector and sequenced by Sanger sequencing (see Table S1 for sgRNA sequences). Finally, to generate newly deficient mESCs for CDC25A or CDC25B, we independently infected ES^{Cas9} cells with at least three different lentiviral supernatants encoding specifically designed sgRNAs targeting either *cdc25a* or *cdc25b*. After infection, the pool of ES^{Cas9} cells, usually infected with a percentage above the 90% of efficiency, was divided in two and either untreated or treated with 2μg/ml of doxycycline for a week to allow gene editing before performing experiments. See the Supplemental Information for a full list of primers and antibodies, as well as the other methods used in this study.

Supplementary Material

Refer to Web version on PubMed Central for supplementary material.

Acknowledgements

We thank Feng Zhang and Kosuke Yusa laboratories for sharing all CRISPR-related plasmids used here through Addgene (#42230, 50946 and 50947), and Edna Fonseca for her comments on the manuscript. Research was funded by Fundación Botín, Banco Santander, through its Santander Universities Global Division and by grants from the Spanish Ministry of Economy and Competitiveness (MINECO) (SAF2011-23753; SAF2014-57791-REDC), Fundació La Marato de TV3, Howard Hughes Medical Institute and the European Research Council (ERC-617840) to OF; by a PhD fellowship from La Caixa Foundation to C.M.; by grants from MINECO to S.R. (RYC2011-09242; SAF2013-49147P, this last project co-financed with European FEDER funds); and by a grant from MINECO (SAF2013-44866-R) to S.O.

References

Beard C, Hochedlinger K, Plath K, Wutz A, Jaenisch R. Efficient method to generate single-copy transgenic mice by site-specific integration in embryonic stem cells. Genesis. 2006; 44:23–28. [PubMed: 16400644]

Bryant HE, Schultz N, Thomas HD, Parker KM, Flower D, Lopez E, Kyle S, Meuth M, Curtin NJ, Helleday T. Specific killing of BRCA2-deficient tumours with inhibitors of poly(ADP-ribose) polymerase. Nature. 2005; 434:913–917. [PubMed: 15829966]

Buisson R, Boisvert JL, Benes CH, Zou L. Distinct but Concerted Roles of ATR, DNA-PK, and Chk1 in Countering Replication Stress during S Phase. Mol Cell. 2015; 59:1011–1024. [PubMed: 26365377]

Cimprich KA, Cortez D. ATR: an essential regulator of genome integrity. Nat Rev Mol Cell Biol. 2008; 9:616–627. [PubMed: 18594563]

Collart MA, Panasenko OO. The Ccr4--not complex. Gene. 2012; 492:42–53. [PubMed: 22027279]

Derenzini E, Agostinelli C, Imbrogno E, Iacobucci I, Casadei B, Brighenti E, Righi S, Fuligni F, Ghelli Luserna Di Rora A, Ferrari A, et al. Constitutive activation of the DNA damage response pathway as a novel therapeutic target in diffuse large B-cell lymphoma. Oncotarget. 2015; 6:6553–6569. [PubMed: 25544753]

Eykelenboom JK, Harte EC, Canavan L, Pastor-Peidro A, Calvo-Asensio I, Llorens-Agost M, Lowndes NF. ATR activates the S-M checkpoint during unperturbed growth to ensure sufficient replication prior to mitotic onset. Cell Rep. 2013; 5:1095–1107. [PubMed: 24268773]

Falck J, Mailand N, Syljuasen RG, Bartek J, Lukas J. The ATM-Chk2-Cdc25A checkpoint pathway guards against radioresistant DNA synthesis. Nature. 2001; 410:842–847. [PubMed: 11298456]

Farmer H, McCabe N, Lord CJ, Tutt AN, Johnson DA, Richardson TB, Santarosa M, Dillon KJ, Hickson I, Knights C, et al. Targeting the DNA repair defect in BRCA mutant cells as a therapeutic strategy. Nature. 2005; 434:917–921. [PubMed: 15829967]

Flynn RL, Cox KE, Jeitany M, Wakimoto H, Bryll AR, Ganem NJ, Bersani F, Pineda JR, Suva ML, Benes CH, et al. Alternative lengthening of telomeres renders cancer cells hypersensitive to ATR inhibitors. Science. 2015; 347:273–277. [PubMed: 25593184]

Foote KM, Blades K, Cronin A, Fillery S, Guichard SS, Hassall L, Hickson I, Jacq X, Jewsbury PJ, McGuire TM, et al. Discovery of 4-{4-[(3R)-3-Methylmorpholin-4-yl]-6-[1-(methylsulfonyl)cyclopropyl]pyrimidin-2-y l}-1H-indole (AZ20): a potent and selective inhibitor of ATR protein kinase with monotherapy in vivo antitumor activity. J Med Chem. 2013; 56:2125–2138. [PubMed: 23394205]

Galaktionov K, Beach D. Specific activation of cdc25 tyrosine phosphatases by B-type cyclins: evidence for multiple roles of mitotic cyclins. Cell. 1991; 67:1181–1194. [PubMed: 1836978]

Halazonetis TD, Gorgoulis VG, Bartek J. An oncogene-induced DNA damage model for cancer development. Science. 2008; 319:1352–1355. [PubMed: 18323444]

Koike-Yusa H, Li Y, Tan EP, Velasco-Herrera Mdel C, Yusa K. Genome-wide recessive genetic screening in mammalian cells with a lentiviral CRISPR-guide RNA library. Nat Biotechnol. 2014; 32:267–273. [PubMed: 24535568]

Kwok M, Davies N, Agathanggelou A, Smith E, Petermann E, Yates E, Brown J, Lau A, Stankovic T. Synthetic lethality in chronic lymphocytic leukaemia with DNA damage response defects by targeting the ATR pathway. Lancet. 2015; 385(Suppl 1):S58. [PubMed: 26312880]

Lecona E, Fernandez-Capetillo O. Replication stress and cancer: it takes two to tango. Exp Cell Res. 2014; 329:26–34. [PubMed: 25257608]

Lopez-Contreras AJ, Fernandez-Capetillo O. The ATR barrier to replication-born DNA damage. DNA Repair (Amst). 2010; 9:1249–1255. [PubMed: 21036674]

Lopez-Contreras AJ, Specks J, Barlow JH, Ambrogio C, Desler C, Vikingsson S, Rodrigo-Perez S, Green H, Rasmussen LJ, Murga M, et al. Increased Rrm2 gene dosage reduces fragile site breakage and prolongs survival of ATR mutant mice. Genes Dev. 2015; 29:690–695. [PubMed: 25838540]

Mailand N, Falck J, Lukas C, Syljuasen RG, Welcker M, Bartek J, Lukas J. Rapid destruction of human Cdc25A in response to DNA damage. Science. 2000; 288:1425–1429. [PubMed: 10827953]

Mankouri HW, Huttner D, Hickson ID. How unfinished business from S-phase affects mitosis and beyond. EMBO J. 2013; 32:2661–2671. [PubMed: 24065128]

Minocherhomji S, Ying S, Bjerregaard VA, Bursomanno S, Aleliunaite A, Wu W, Mankouri HW, Shen H, Liu Y, Hickson ID. Replication stress activates DNA repair synthesis in mitosis. Nature. 2015; 528:286–290. [PubMed: 26633632]

Murga M, Campaner S, Lopez-Contreras AJ, Toledo LI, Soria R, Montana MF, D'Artista L, Schleker T, Guerra C, Garcia E, et al. Exploiting oncogene-induced replicative stress for the selective killing of Myc-driven tumors. Nat Struct Mol Biol. 2011; 18:1331–1335. [PubMed: 22120667]

Peng CY, Graves PR, Thoma RS, Wu Z, Shaw AS, Piwnica-Worms H. Mitotic and G2 checkpoint control: regulation of 14-3-3 protein binding by phosphorylation of Cdc25C on serine-216. Science. 1997; 277:1501–1505. [PubMed: 9278512]

Prevo R, Fokas E, Reaper PM, Charlton PA, Pollard JR, McKenna WG, Muschel RJ, Brunner TB. The novel ATR inhibitor VE-821 increases sensitivity of pancreatic cancer cells to radiation and chemotherapy. Cancer Biol Ther. 2012; 13:1072–1081. [PubMed: 22825331]

Prister SX, Markkanen E, Jiang J, Sarkar S, Woodcock M, Orlando G, Mavrommati I, Pai C, Zalmas L, Drobinitzky N, et al. Inhibiting WEE1 Selectively Kills Histone H3K36me3-Deficient Cancers by dNTP Starvation. Cancer Cell. 2015; 28:557–568. [PubMed: 26602815]

Ray D, Kiyokawa H. CDC25A phosphatase: a rate-limiting oncogene that determines genomic stability. Cancer Res. 2008; 68:1251–1253. [PubMed: 18316586]

Reaper PM, Griffiths MR, Long JM, Charrier JD, Maccormick S, Charlton PA, Golec JM, Pollard JR. Selective killing of ATM- or p53-deficient cancer cells through inhibition of ATR. Nat Chem Biol. 2011; 7:428–430. [PubMed: 21490603]

Russell P, Nurse P. cdc25+ functions as an inducer in the mitotic control of fission yeast. Cell. 1986; 45:145–153. [PubMed: 3955656]

Sanchez Y, Wong C, Thoma RS, Richman R, Wu Z, Piwnica-Worms H, Elledge SJ. Conservation of the Chk1 checkpoint pathway in mammals: linkage of DNA damage to Cdk regulation through Cdc25. Science. 1997; 277:1497–1501. [PubMed: 9278511]

Santos MA, Faryabi RB, Ergen AV, Day AM, Malhowski A, Canela A, Onozawa M, Lee JE, Callen E, Gutierrez-Martinez P, et al. DNA-damage-induced differentiation of leukaemic cells as an anti-cancer barrier. Nature. 2014; 514:107–111. [PubMed: 25079327]

Sarmento LM, Povoa V, Nascimento R, Real G, Antunes I, Martins LR, Moita C, Alves PM, Abecasis M, Moita LF, et al. CHK1 overexpression in T-cell acute lymphoblastic leukemia is essential for proliferation and survival by preventing excessive replication stress. Oncogene. 2015; 34:2978–2990. [PubMed: 25132270]

Schoppy DW, Ragland RL, Gilad O, Shastri N, Peters AA, Murga M, Fernandez-Capetillo O, Diehl JA, Brown EJ. Oncogenic stress sensitizes murine cancers to hypomorphic suppression of ATR. J Clin Invest. 2012; 122:241–252. [PubMed: 22133876]

Toledo LI, Altmeyer M, Rask MB, Lukas C, Larsen DH, Povlsen LK, Bekker-Jensen S, Mailand N, Bartek J, Lukas J. ATR prohibits replication catastrophe by preventing global exhaustion of RPA. Cell. 2013; 155:1088–1103. [PubMed: 24267891]

Toledo LI, Murga M, Zur R, Soria R, Rodriguez A, Martinez S, Oyarzabal J, Pastor J, Bischoff JR, Fernandez-Capetillo O. A cell-based screen identifies ATR inhibitors with synthetic lethal properties for cancer-associated mutations. Nat Struct Mol Biol. 2011; 18:721–727. [PubMed: 21552262]

Vendetti FP, Lau A, Schamus S, Conrads TP, O'Connor MJ, Bakkenist CJ. The orally active and bioavailable ATR kinase inhibitor AZD6738 potentiates the anti-tumor effects of cisplatin to resolve ATM-deficient non-small cell lung cancer in vivo. Oncotarget. 2015

Europe PMC Funders Author Manuscripts

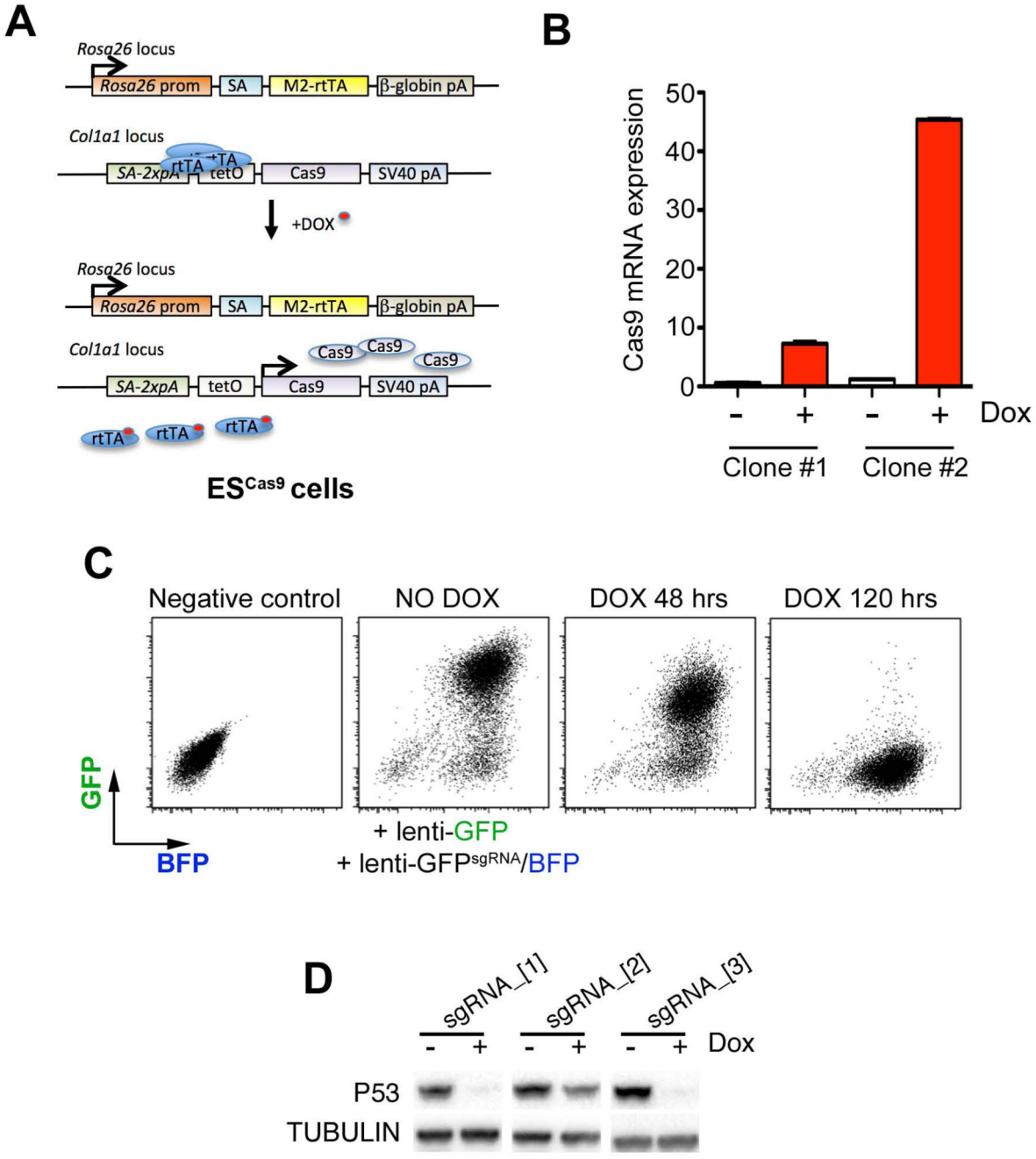

Figure 1. Efficient and Dox-inducible gene knockouts in ES^{Cas9} cells.

(A) Scheme illustrating the two-allele system used for the generation of ES^{Cas9} cells. In this previously described system(Beard et al., 2006), the Cas9 cDNA is placed under the control of a tet-responsible sequence (tetO) at the *Col1a1* locus. At the same time, the reverse tetracycline-controlled transactivator (rtTA) is expressed from the *Rosa26* locus, providing Dox-inducible-activation of Cas9 expression.

(B) Levels of Cas9 mRNA evaluated by RT-PCR (normalized to levels of GAPDH mRNA) in the 2 clones of ES^{Cas9} cells used in this study. The high stringency of the system prevents

cleavage in the absence of Dox. Data are represented as mean ± s.d. (n=3). See also Figure S1A,B.

(C) FACS analysis illustrating the loss of GFP signal in ES^{Cas9} cells that were made GFP positive by infection with a lentiviral construct expressing GFP, and simultaneously infected with a lentivirus expressing a *Gfp*-targeting sgRNA together with BFP. Doubly infected cells are thus BFP and GFP positive, and gradually lose GFP expression after the addition of Dox. See also Figure S1C.

(D) Western blot illustrating the Dox-dependent loss of P53 expression observed in ES^{Cas9} cells that were infected with lentiviruses expressing 3 independent *P53*-targeting sgRNAs. TUBULIN levels are shown as a loading control. Dox was used at 2 μg/ml.

Europe PMC Funders Author Manuscripts

Europe PMC Funders Author Manuscripts

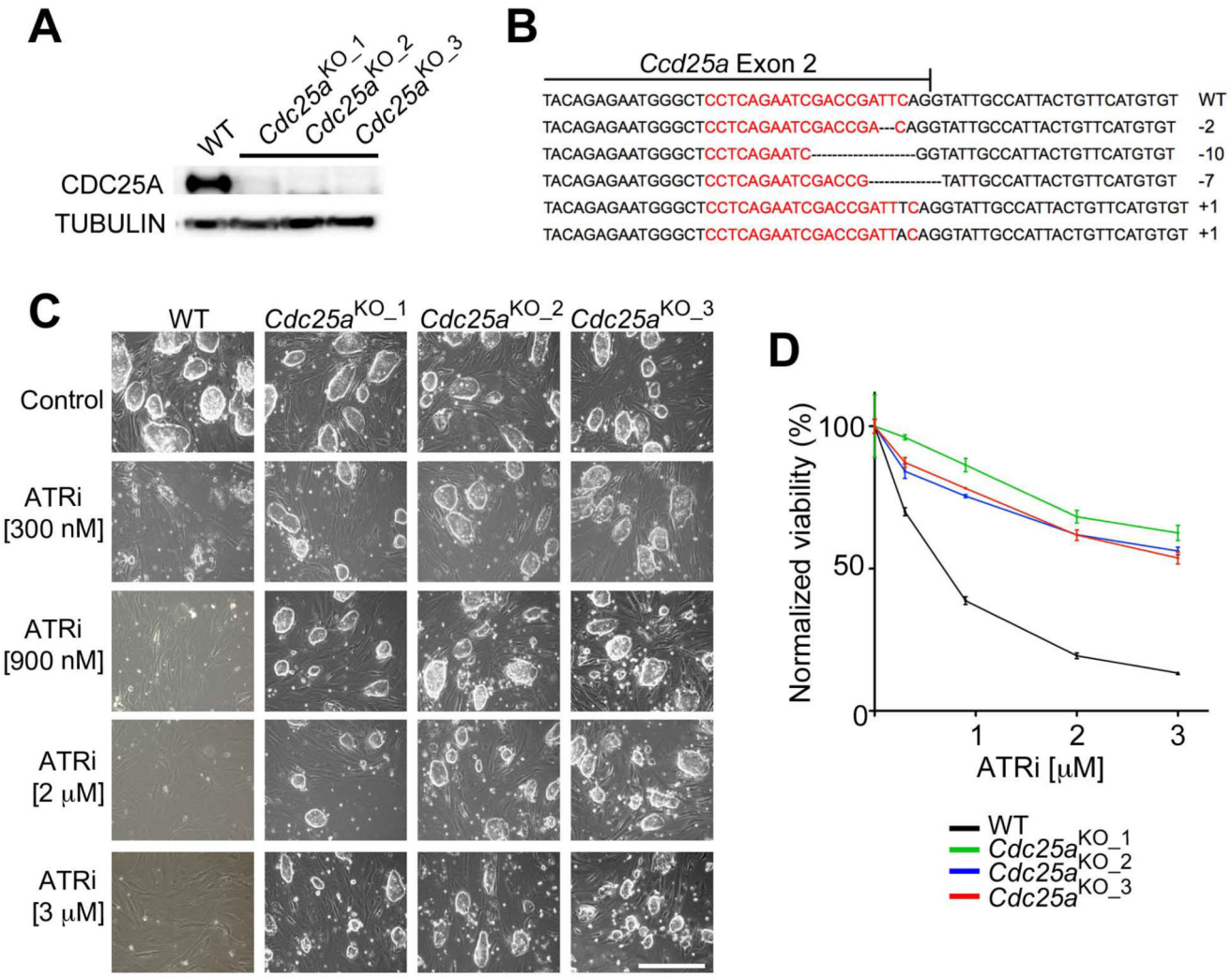

Figure 2. Resistance to ATR inhibition in CDC25A-deficient ES^{Cas9} cells.

(A) Western blot illustrating the loss of CDC25A expression in 3 independent ATRi-resistant clones.

(B) Examples of the mutations in *Cdc25a* identified in ATRi-resistant ES^{Cas9} cells shown in (A). Note that all mutations include small insertions or deletions that change the reading frame in exon 2, precisely at the 3' of the sgRNA sequence (in red).

(C) Representative pictures of the resistance to ATRi observed in CDC25A-deficient ES^{Cas9} cells exposed to the compound for 72 hr. ES cells are grown on top of a feeder layer of growth-arrested MEF, which are unaffected by the treatment. Scale bar (white) indicates 25 μm.

(D) XTT viability assay in wild type and CDC25A-deficient ES^{Cas9} cells exposed to ATRi for 24 hr at the indicated doses. Data are representative of 3 independent experiments. Error bars indicate s.d. See also Figure S2.

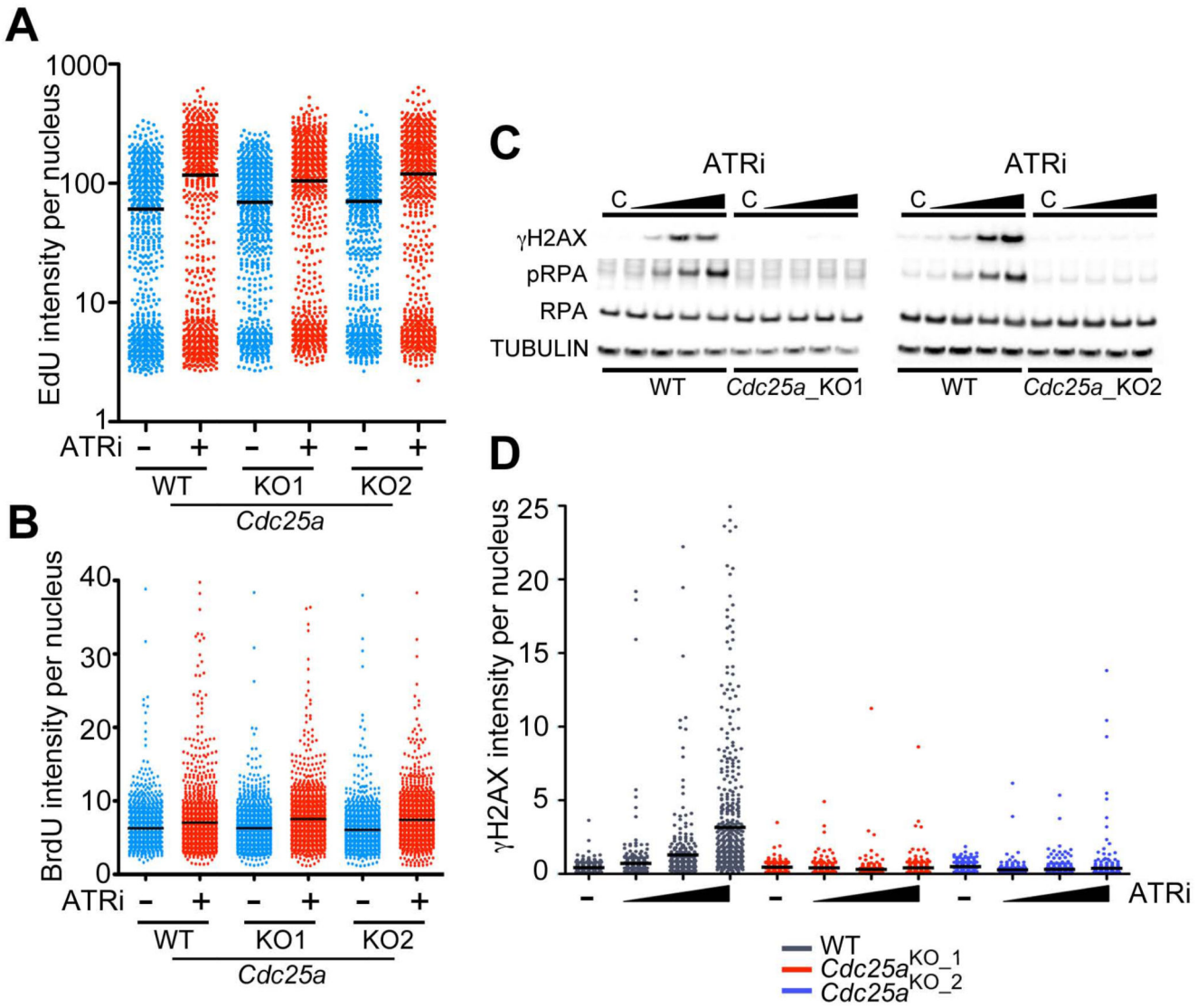

Figure 3. ATR inhibition generates RS but not DSB in CDC25A-deficient cells.

(A) HTM analysis of the EdU signal per individual nucleus in wild type (WT) and CDC25A-deficient ES^{Cas9} cells exposed to ATRi for 1 hr (900 nM).

(B) HTM analysis of the BrdU signal accumulated in ssDNA per individual nucleus in wild type (WT) and CDC25A-deficient ES^{Cas9} cells exposed to ATRi for 4 hr (900 nM).

(C) WB illustrating the levels of H2AX (γH2AX) and RPA (S4/8) phosphorylation in WT and CDC25A-deficient ES^{Cas9} cells exposed to ATRi for 4 hr (0, 0.3, 0.9, 2 and 3 μM). TUBULIN and total RPA levels are shown as loading controls.

(D) HTM analysis of the γH2AX signal per individual nucleus in WT and CDC25A-deficient ES^{Cas9} cells treated (or not) with ATRi (0.3, 0.9 and 2 μM; 4 hr). See also Figure S3.

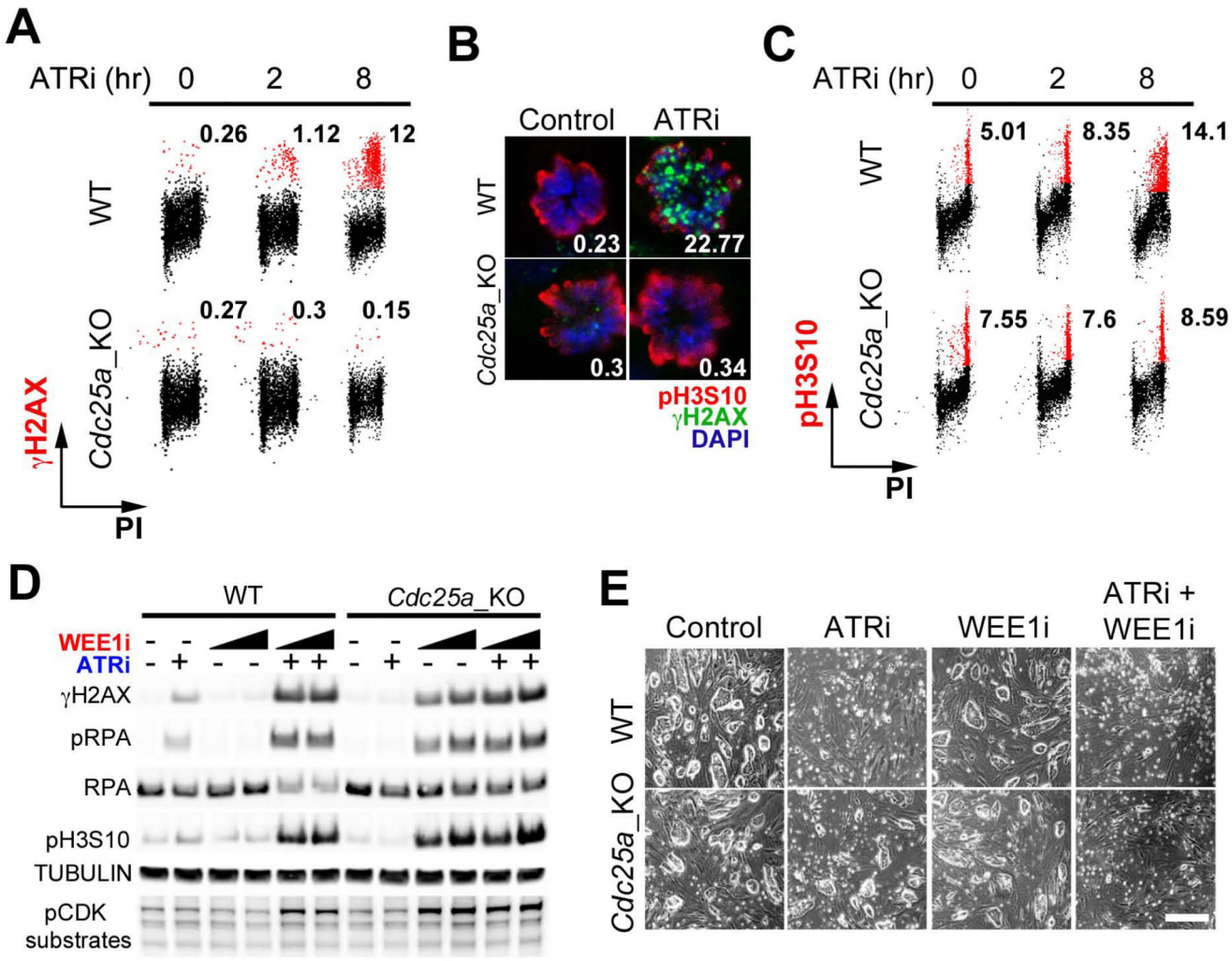

Figure 4. ATRi induces premature mitotic entry and DNA breakage in a CDC25A-dependent manner.

(A) Representative FACS profiles showing the distribution of γH2AX-positive cells (*x*, DNA content; *y*, γH2AX) of WT and CDC25A-deficient ES^{Cas9} cells exposed to ATRi (900 nM) for the indicated times. Numbers indicate the percentage of γH2AX-positive cells (red) in each case.

(B) Representative image of the presence of DSBs in mitotic ES^{Cas9} cells exposed to ATRi for 4 hr (300 nM). Mitotic cells were identified by antibodies against pH3S10 (red). DSBs were identified by γH2AX (green) foci. DAPI was used to stain DNA. Numbers in white indicate the percentage of pH3S10-positive cells presenting γH2AX foci. Scale bar (white) indicates 2.5 μm.

(C) Representative FACS profiles showing the distribution of pH3S10-positive cells (*x*, DNA content; *y*, pH3S10) of WT and CDC25A-deficient ES^{Cas9} cells exposed to ATRi (900 nM) for the indicated times. Numbers indicate the percentage of pH3S10-positive cells (red) in each case.

(D) WB illustrating the levels of H2AX (γH2AX), RPA (S4/8) and H3 (S10) phosphorylation in WT and CDC25A-deficient ES^{Cas9} cells exposed to ATRi (300 nM)

and/or WEE1i (100 or 300 nM) for 4 hr. An antibody detecting phosphorylated CDK substrates was also used as measure of overall CDK activity. TUBULIN and total RPA levels are shown as loading controls.

(E) Representative pictures of cultures of WT and CDC25A-deficient ES^{Cas9} cells exposed to ATRi (300 nM) and/or WEE1i (100 nM) for 72 hr. Scale bar (white) indicates 25 μm. See also Figure S4.

Europe PMC Funders Author Manuscripts